

Cyclical Mutation of Stator and Rotor Designs and Their Impact to the Acoustic Behavior of Induction Motor

C. Grabner

Abstract – The acoustic sound level caused as secondary effect during the electrical energy conversion is often perceived as an unwelcome noise emitted into the enclosing surrounding. In order to verify design aspects for reducing such undesirable noise emission suggested combinations of novel motor topologies are analyzed.

I. INTRODUCTION

As the motor design process has to consider multi-physical effects, such as e.g. electrical, thermal and mechanical aspects, a very deep and complex analysis has to take place in order to find the best technical and commercial choice for the product. Thus, extended investigations to the acoustic behavior of the complete speed variable induction drive system, as it is schematically depicted in Fig.1, have been performed in the lab to obtain reproducible results with high accuracy.

Main interest is thereby given to the influence of the complete mechanical induction motor design to the almost manifold acoustic response under sinusoidal power supply. This includes the investigation of unexpected effects even caused by passing critical speed values which are corresponding to mechanical resonance frequencies. To take remedial measures, totally-closed stator topologies and rotor skewing opportunities, have been deeply investigated in a comparatively manner.



Figure 1: A 750W 4-pole squirrel cage induction motor in FS80.

Manuscript received March 25, 2008.

Christian Grabner is with the Research and Development Department of Drive Systems, Siemens AG, Frauenauracherstrasse 80, D-91056 Erlangen, Germany, (phone: +49 162 2515841, e-mail: grabner.christian@siemens.com).

II. PHYSICAL FUNDAMENTALS OF ACOUSTIC NOISE

Sound is the mechanical vibration of a gaseous medium through which the energy is transferred away from the source by progressive sound waves. Whenever an object vibrates, a small portion of the energy involved is lost to the surrounding area as unwanted sound – the acoustic noise [1,2].

A. Sound power

Any source of noise is commonly characterized by the emitted sound power, measured in Watt. This fundamental physical property of the source itself is often known as absolute parameter for the acoustic output.

The sound power can be found conceptually by adding the product of the areas times the acoustic intensities for the areas on any hypothetical surface that contains the source. Since equipment for measuring of acoustic intensity is generally not available, sound power inevitably has to be determined indirectly by taking the spatial average of the sound pressure squared measured on equal areas on the surrounding surface.

B. Sound pressure level in decibel

As the acoustic intensity, the power passing through a unit area in space, is proportional in the far field to the square of the sound pressure, a convenient scale for the acoustic measurement can be defined as sound pressure level

$$L_p(t) = 10 \log \left(\frac{p(t)}{p_0} \right)^2 = 20 \log \left(\frac{p(t)}{p_0} \right), \quad (1)$$

in decibel, with p_0 as the reference sound pressure of 20 μPa . The measured sound pressure $p(t)$ in (1) depends on many insecure factors, such as e.g. orientation and distance of receiver, temperature and velocity gradients inside the involved medium.

The analysis of (1) in the frequency domain is fortunately done with the discrete fast Fourier-analysis. Therefore, the time-periodical signal (1) is sampled as $L_{p,n}$ and further processed at a distinct number of N samples as

$$\hat{L}_{p,v} = \sum_{n=0}^{N-1} L_{p,n} e^{-j(2\pi n/N)v}, \quad v = 0, 1, 2, \dots, N-1 \quad (2)$$

in order to obtain the Fourier coefficients $\hat{L}_{p,v}$ of the interested frequency-domain.

III. SOUND PRESSURE LEVEL AND HUMAN HEARING

Unfortunately, no simple relationship exists between the measured physical sound pressure level and the human perception of the same sound. The treatment of acoustic noise and its effects is therefore a complicated problem, which must take a wide variety of parameters into account to achieve good correlations between measurement and the resultant human reaction.

C. Human hearing mechanism

The quietest sound at 1000 Hz which can be heard by the average person is found in Fig.2 to be about $20 \mu\text{Pa}$ and this value has been standardized as the nominal hearing threshold for the purpose of sound level measuring. At the other end of the scale the threshold of pain occurs at a sound pressure of approximately 100 Pa.

An inspection of Fig.2 shows that a pure tone having a sound pressure level of e.g. 20 dB and a frequency of 1000 Hz is plainly audible, whereas one having the same sound pressure level but a frequency of 100 Hz is well below the threshold of audibility and cannot be heard at all.

D. Loudness level in phon

The loudness of a pure tone of constant sound pressure level, perhaps the simplest acoustic signal of all, varies with its frequency, even though the sound pressure may be the same in every case.

Although our hearing mechanism is not well-adapted for making quantity measurements of the relative loudness of different sounds, there is a fair agreement between observers, when two pure tones of different frequencies appear to be equally loud. It is therefore possible to establish in Fig.2 contour plots of equal loudness in phon. These subjective felled loudness curves are obtained by alternately sounding a reference tone of 1000 Hz and a second tone of some other frequency. The intensity level of the second tone is then adjusted to the value that makes the two tones appear equally loud.

A pure tone having a frequency of 100 Hz and a sound pressure level of about 35 dB sounds as loud as a pure 1000 Hz tone whose intensity level is 20 dB, and hence the loudness level of the 100 Hz tone is by definition 20 phon. The 1000 Hz frequency is thus the reference for all loudness measurements, and all contours of equal loudness expressed in phon have the same numerical value as the sound pressure level in dB at 1000 Hz.

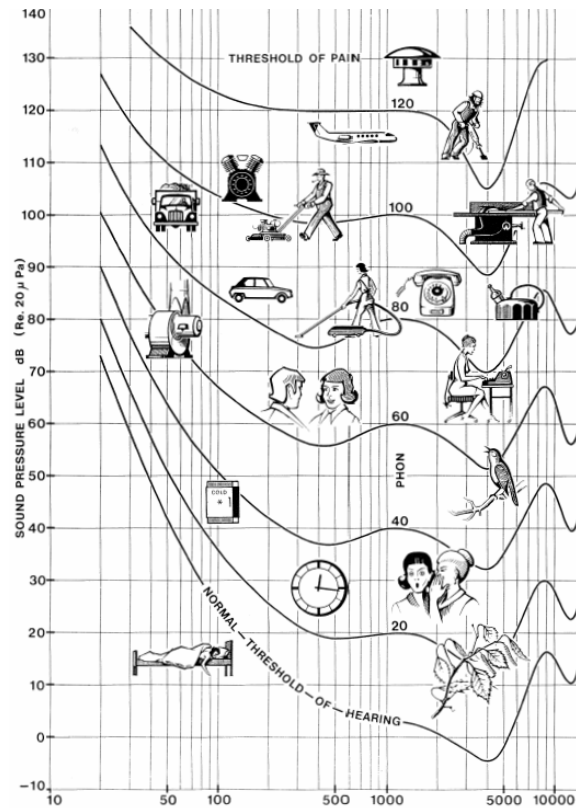


Figure 2: Typical sound pressure levels in dB and equal loudness levels in phon for different noise sources.

E. Weighing the sound pressure level

Due to the human ears assessment of loudness, the defined purely physical sound pressure terminus has to be modified by an implicit weighting process in a way which corresponds to the more complex response of the human being. Therefore, among several possibilities, distinguished by B, C, D, E or SI-weighting in Fig.3, the A-weighted level has been found to be the most suitable for modifying the frequency response to follow approximately the equal loudness of 20 phon in Fig.2.

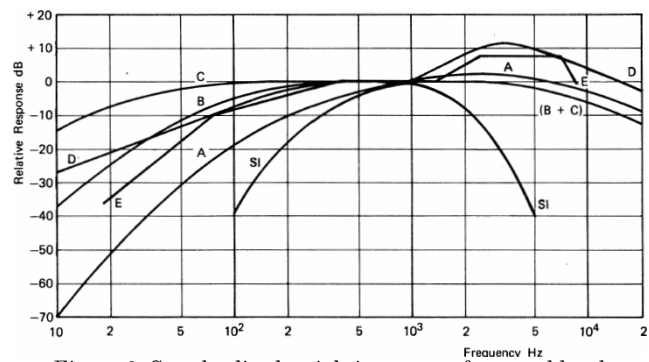


Figure 3: Standardized weighting curves for sound level measurement.

IV. ACOUSTIC NOISE MEASUREMENT

Laboratory methods for testing noise specifications are usually very exhaustive, because the equipment and measurement procedures are subjected to international standards in order to guarantee the uniformity and quality of the measured results [3,4].

F. Semi-anechoic chamber

The most accurate values of sound power levels are naturally determined in free field environment conditions. This is not practicable if heavily test specimens such as electrical drives are used. Thus, they are usually placed at a hard reflecting surface with absorption coefficients less than 0.06 in so called semi-anechoic chambers. A typical lab equipped with absorbing walls and several microphones is shown in Fig.4.

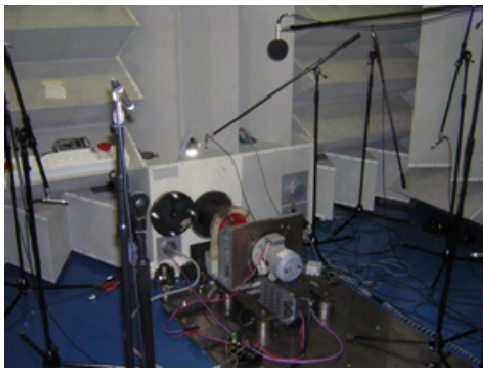


Figure 4: Schematically lab set-up for the acoustic noise measurement according to DIN EN ISO 3744.

According to DIN EN ISO 3744 a fictive rectangular parallelepiped, which is schematically depicted in Fig.5 is applied for defining the exact spatial position of the used nine microphones. Thereby, the total surface of the test box is calculated as

$$S = 4(ab + bc + ca) , \\ a = 0.5l_1 + d , b = 0.5l_2 + d , c = l_3 + d . \quad (3)$$

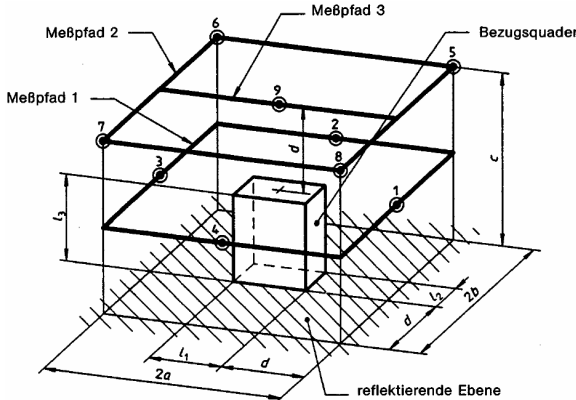


Figure 5: Microphone positions inside a semi-anechoic chamber.

The noise source to be measured is situated in Fig.5 in the centered area, which is characterized by the length l_1 , the width l_2 and the height l_3 . The other associated geometric distances in Fig.5 are thereby restricted by $l_1 \leq d$, $l_2 \leq d$ and $l_3 \leq 2d$. The value for the distance d is about 1 m.

G. Measured continuous A-weighted sound pressure level at each microphone

With a wide variety of electrical circuits to condition, weight and integrate the signal path, the analysis section of the system shown in Fig.6 is usually the most complex.

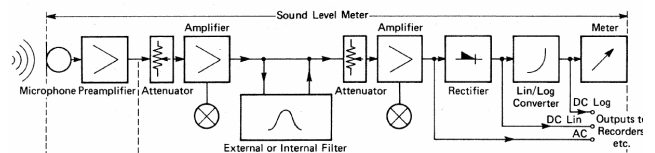


Figure 6: Typical block diagram of a noise measuring system.

The A-weighted sound pressure level

$$L_{pA}(t) = 10 \log \left(\frac{p_A(t)}{p_0} \right)^2 , \quad (4)$$

expressed in dB(A), is directly accessible to measurement by incorporating an according filter, as shown in Fig.6. It correlates therefore extremely well with the subjective human response. The term $p_A(t)$ is denoted as the A-weighted instantaneous acoustic sound pressure $p(t)$. The analysis of (4) in the frequency domain takes advantage use of the fast Fourier transformation (2).

Treating time rather than frequency as the important variable, the A-weighted level (4) may be integrated over the measured time-period T as

$$\bar{L}_{pA} = \frac{1}{T} \int L_{pA}(t) dt , \quad (5)$$

in order to give the A-weighted mean of the steady continuously time dependent signal $L_{pA}(t)$.

H. Equivalent A-weighted surface sound pressure level over all microphones

The equivalent surface sound pressure level is obtained from the A-weighted and time-averaged signals (5) at a total number of N microphones as

$$\bar{\bar{L}}_{pA} \approx \frac{1}{N} \sum_{i=1}^N \bar{L}_{pAi} - K_{1A} - K_{2A} . \quad (6)$$

The first correction coefficient K_{1A} in (6) takes implicit account of eventually disturbing A-weighted environmental noise. The second correction coefficient K_{2A} in (6) considers the A-weighted reflection or absorption of sound with regard to the surface sound power level.

I. Equivalent A-weighted surface sound power level

The measured equivalent A-weighted surface sound power level could be directly obtained from (6) with the geometric relation (3) in accordance to

$$\bar{L}_{wA} = \bar{L}_{pA} + 10 \log \left(\frac{S}{S_0} \right), \quad (7)$$

whereby S_0 denotes the reference area of 1 square meter. Thus the difference between the spatial averaged sound pressure level (6) and power level (7) is constant. With an area S_0 of 14.3 m^2 in case of the used set-up in Fig.5, the constant term in (7) is determined as 11 dB.

V. CYCLICAL MUTATION OF STATOR AND ROTOR PART COMBINATION

The stator part of a squirrel cage induction motor is typically manufactured so far with semi-closed stator slots [5,6]. However, continual progress in the industrial automation process allows the utilization of a novel stator construction with totally-closed stator slots as shown in Fig.7. The squirrel cage rotor could alternatively be built up with a skewed or even non-skewed rotor as depicted in Fig.8. Based on the proposed different stator and rotor components, four motor designs, as listed in Table I, have been consecutively tested with regard to their suitability for acoustic noise minimization.

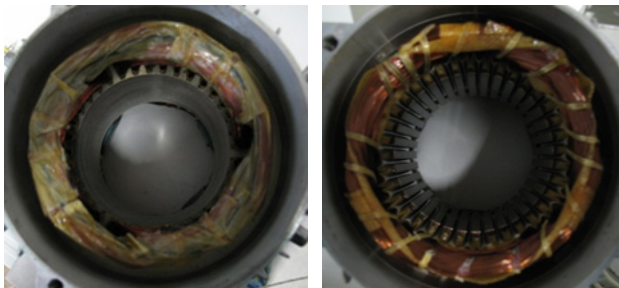


Figure 7: Stator design with totally-closed (left) and semi-closed (right) stator slots.

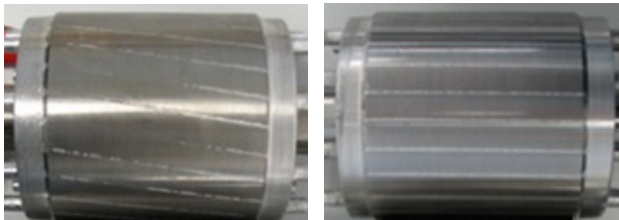


Figure 8: Skewed (left) and un-skewed (right) rotor.

TABLE I

Combination	Stator slot design	Rotor design
Motor ①	Totally-closed	skewed
Motor ②	Totally-closed	un-skewed
Motor ③	Semi-closed	un-skewed
Motor ④	Semi-closed	skewed

VI. DIRECT COMPARISON OF SOUND PRESSURE LEVELS FOR DIFFERENT MOTOR DESIGNS

All investigated motor designs are operated at the rated electrical voltage level of 400 V. They have a rated power of approximately 750 W at the nominal speed of about 1395 rpm. As all listed samples in Table I are assisted with the same motor fan, a direct comparison of the acoustic tests results is feasible.

The noise measurement has been carried out for each motor design over a wide speed range beginning from the lower value of 500 rpm up to rated-speed of 1395 rpm at constant mechanical rated-torque of 5 Nm. Within increasing higher speed ranges, the drive works in the field weakening range and so the load has been continuously reduced.

After reaching the physically quasi-steady operational state for each adjusted speed value, the measured data set has been stored. Thus, purely dynamic acoustic noise in fact of a transient real-time run-up is herewith not considered.

J. Evaluation of design impacts to the equivalent sound pressure level

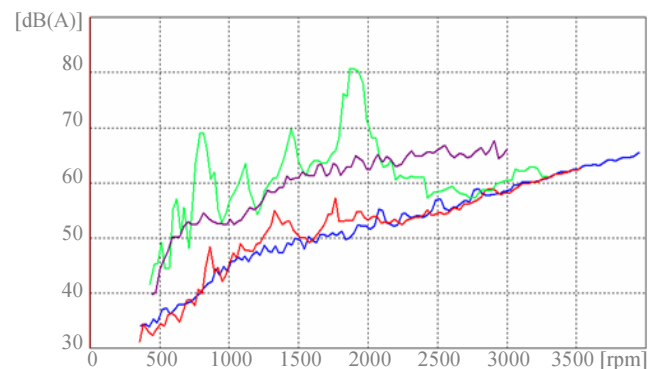


Figure 9: Measured sound pressure level versus speed for the motor ① (blue), motor ② (red), motor ③ (green) and motor ④ (violet) at sinusoidal power supply and no-load.

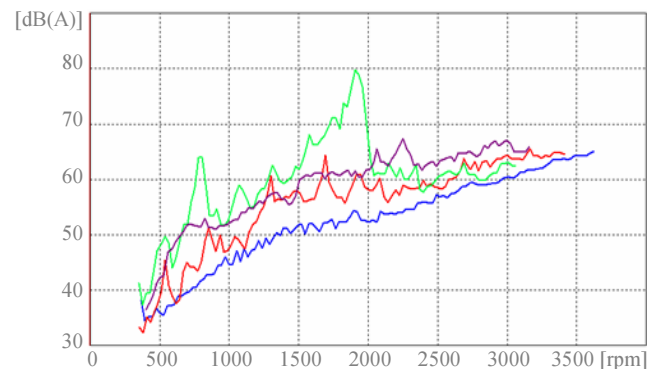


Figure 10: Measured sound pressure level versus speed for the motor ① (blue), motor ② (red), motor ③ (green) and motor ④ (violet) at sinusoidal power supply and rated-load.

The depicted sound pressure level courses in Fig.9 and Fig.10, which are representing the skewed rotor designs ① and ④, show a very smooth and continuous track behavior, which fortunately avoids extensively noise peaks over the total speed range. Thus, the utilization of the standard skewing technology avoids the generation of undesired significant noise peak over the complete speed range.

As obviously from Fig.9 and Fig.10, the course of the proposed novel motor combination ① has advantageously the lowest sound pressure level in comparison to the usually design ④ at several speed values. The introduced novel motor topology of the standard squirrel cage induction motor with totally-closed slot tips is therefore suitable to reduce undesired noise emission not only at the nominal speed of 1395 rpm. The emitted noise of the proposed motor design ① is reduced by the amount of 10 db at no-load in Fig.9 and about 8 db at rated-load in Fig.10 in comparison to the state of the art design ④.

Contrarily, in case of both test objects ② and ③, a very discontinuous and even speed sensitive sound level behaviors characterized by some very distinct noise peaks is found from Fig.9 and Fig.10.

Especially the varying operational state from no-load to rated-load causes extended magnetic saturation effects within the totally-closed stator tooth tip regions. This fact has, in dependency on the motor design ② or ③ unexpected inverse impacts to the emitted noise levels. There are some interesting secondary aspects occurring at higher speed ranges. Considering the test object ③, the maximal occurring peak of 81 dB in Fig.9 at 1842 rpm is slightly reduced at the same speed value to 79 dB in Fig.10. A completely contrarily observation could be for motor ②. The noise peak of 55 dB at 1670 rpm at no-load is significantly shifted to much higher levels with arising additional peaks of 62 dB at the same speed in case of the rated-load condition in Fig.10.

VII. FAST FOURIER SOUND PRESSURE SPECTRUM FOR EACH MOTOR DESIGN AT RATED-LOAD

The description of the time-depended sound pressure in the frequency domain allows a deeper inside into the fundamental aspects of noise generation. The harmonic sound pressure frequency components of the motors ① to ④ are depicted in Fig.11 to Fig.14 over the extended speed range.

The utilization of a skewed rotor type in motor ① obviously results in Fig.11 in green shaded lower range spectral magnitudes. Contrarily, the test results of the skewed design ④ given in Fig.14 show a high 58 dB peak at the frequency of 1900 Hz.

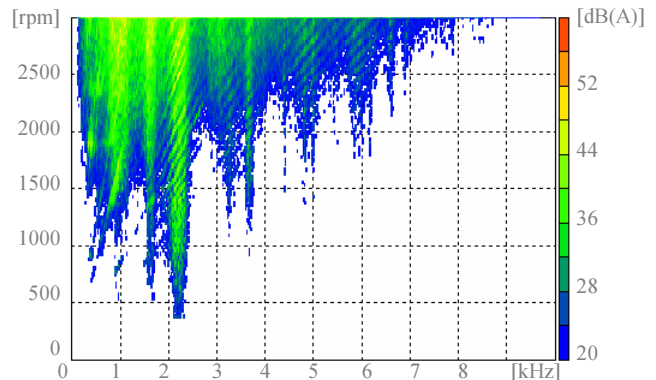


Figure 11: FFT of the sound pressure level for motor ① at rated-load depicted for the speed range 500-3000 rpm.

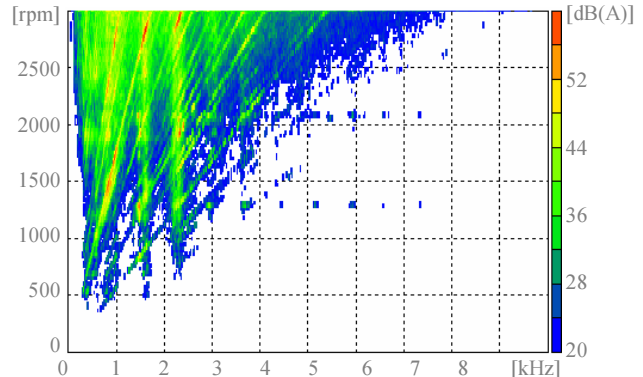


Figure 12: FFT of the sound pressure level for motor ② at rated-load depicted for the speed range 500-3000 rpm.

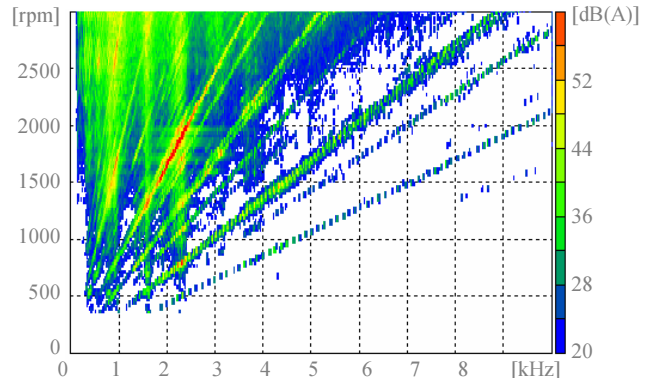


Figure 13: FFT of the sound pressure level for motor ③ at rated-load depicted for the speed range 500-3000 rpm.

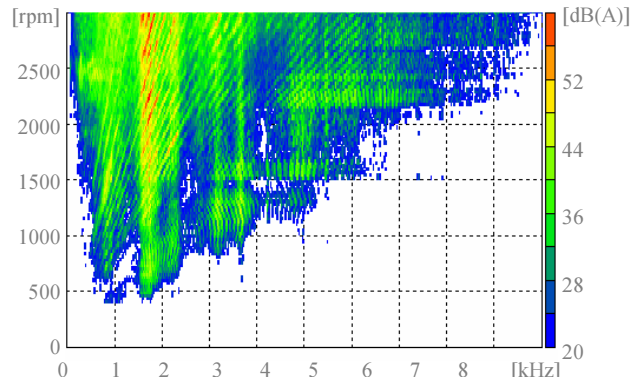


Figure 14: FFT of the sound pressure level for motor ④ at rated-load depicted for the speed range 500-3000 rpm.

A distinct noise peak of electromagnetic origin of the un-skewed design ② is visible in Fig.12 at the speed 1670 rpm with the frequency of 940 Hz.

Some very distinct spectral components due to stator slot harmonics of motor ③ at the speed of 1900 rpm could be identified in Fig.13 with magnitudes of 59 dB at the surrounding of the single frequency of 2300 Hz.

VIII. CONCLUSION

The evaluation of distinct influences to the acoustic noise emission of industrial standard squirrel cage motors is fairly a very sensitive and complex topic.

The performed comparatively measurement of the speed dependent equivalent continuous A-weighted surface sound pressure level gives a good overview about the principal design influences. The main focus at standard drives is thereby only given to the occurring noise peaks at the interested nominal speed.

The modification of induction motors, which are commonly assisted by skewed rotors, by applying novel totally-closed stator slot designs, is the most favorable possibility for reducing the emitted acoustic noise level. Fortunately, the magnetic utilization could almost be kept equal.

If the rotor is alternatively manufactured in an un-skewed kind, the acoustic noise emission would reach the same level as with utilized semi-closed slots in combination with a skewed rotor.

REFERENCES

- [1] L.E. Kinsler and A.R. Frey, *Fundamentals of acoustics*, John Wiley & Sons, Inc.: New York/London, 1962.
- [2] M. Bruneau, *Fundamentals of acoustics*, ISTE: London, 2006.
- [3] J.R. Hassall and K. Zaveri, *Acoustic noise measurement*, Brüel & Kjaer: Denmark, 1979.
- [4] DIN EN ISO 3744, "Determination of sound power levels of noise sources using sound pressure – Engineering method in an essentially free field over a reflecting plane," Deutsches Institut für Normung e.V., 1995.
- [5] H. Jordan, *Der geräuscharme Elektromotor*, Verlag W. Girardet: Essen, 1950.